mathematics

MDPI

Article

The Collocation Method Based on the New Chebyshev Cardinal Functions for Solving Fractional Delay Differential Equations

Haifa Bin Jebreen [1,*] and Ioannis Dassios [2]

[1] Department of mathematics, College of Science, King Saud University, P.O. Box 2455, Riyadh 11451, Saudi Arabia
[2] Faculty of Engineering, Aristotle University of Thessaloniki, 541 24 Thessaloniki, Greece; ioannisdassios@gmail.com
* Correspondence: hjebreen@ksu.edu.sa

Abstract: The Chebyshev cardinal functions based on the Lobatto grid are introduced and used for the first time to solve the fractional delay differential equations. The presented algorithm is based on the collocation method, which is applied to solve the corresponding Volterra integral equation of the given equation. In the employed method, the derivative and fractional integral operators are expressed in the Chebyshev cardinal functions, which reduce the computational load. The method is characterized by its simplicity, adherence to boundary conditions, and high accuracy. An exact analysis has been provided to demonstrate the convergence of the scheme, and illustrative examples validate our investigation.

Keywords: Chebyshev cardinal functions; Lobatto grid; delay differential equations; collocation method

MSC: 54A25; 65L60; 34Kxx; 34A08

Citation: Jebreen, H.B.; Dassios, I. The Collocation Method Based on the New Chebyshev Cardinal Functions for Solving Fractional Delay Differential Equations. *Mathematics* **2024**, *12*, 3388. https://doi.org/10.3390/math12213388

Academic Editors: Faïçal Ndaïrou and Delfim F. M. Torres

Received: 23 September 2024
Revised: 27 October 2024
Accepted: 28 October 2024
Published: 30 October 2024

1. Introduction

Even though fractional calculations have a long history, their use has received much attention from researchers in recent years. The widespread applications of this concept across engineering, physics, and mathematics have led to the development and application of numerous accurate models for understanding physical phenomena [1–4]. It is impossible to deny the significance of fractional differential equations in this context. Several analytical and numerical methods have been developed and applied to find the solution of fractional differential equations. Here, some of them can be mentioned, such as the wavelet method [5–7], collocation method [8–10], multi-step methods [11], finite element-meshfree method [12], B-spline collocation method [13], Adomian decomposition [14], finite element method [15], implicit integration factor method [16], and adaptive-grid technique [17].

Delay differential equations (DDEs) are a significant and practical branch of differential equations with many applications in population dynamics, bioengineering, chemistry, control systems, physics, electrochemistry, etc. [14,18–21]. Among the available methods, numerical approaches have always been useful and effective techniques for solving differential equations. Saray et al. [22] applied the wavelet Galerkin method to solve the DDEs with an effective and novel algorithm. Mohammadzadeh et al. [23] have solved the DDEs by applying new hybrid functions. The time-delay systems were considered and studied by an efficient algorithm relying on a hybrid function [24]. We refer the readers to [25–30] to study more related work in this context.

According to the aforementioned reviewed contents, considering fractional DDEs can be an important subject for study. The modeling of real-world problems can be more accurate by including fractional derivatives and delays. Fractional DDEs have numerous applications in bioengineering, physics, population dynamics, control systems, electrochemistry, chemistry, finance, etc. [31,32]. In bioengineering, fractional derivatives

enhance our understanding of the dynamics that take place in biological tissues. This understanding is valuable for studying magnetic resonance imaging of complex, porous, and heterogeneous materials and nuclear magnetic resonance found in both living and nonliving systems [33].

In this work, the fractional DDEs of the form

$$\begin{aligned} {}^{c}\mathcal{D}_t^{\kappa}(u)(t) &= \eta_1 u(t-d) + \eta_2 u(t) + g(t), \quad t \in [0,b], d \in [0,1), \kappa \in (0,1), \\ u(t) &= w(t), \qquad t \in [-d,0), \\ u(0) &= u_0, \end{aligned} \tag{1}$$

is considered. Here η_1, η_2 are constants, g is a continuous function, and $w(t)$ is a delay condition. The fractional derivative in this model is considered to be of the Caputo type. The existence and uniqueness of solutions to this problem were investigated in [34]. Several numerical methods can be found in the literature to solve this equation. In the sequel, some of them will be mentioned. The Adams method is used for solving this equation [35]. Singh [33] applied an efficient algorithm based on third-kind Chebyshev polynomials to find the numerical solution of Equation (1). In [36], the authors used the collocation method, relying on the Genocchi wavelet to solve this equation. The fractional DDEs have been solved using a new algorithm and Jacobi polynomials [37]. A new decomposition scheme [38] is studied to find the solution of Equation (1). The error analysis is also investigated in this work. The fractional DDEs with the Riemann–Liouville and Caputo derivatives are studied in [39]. This work employs the finite difference-based approximation and interpolation-based approximation for the Riemann–Liouville and Caputo derivatives to introduce the higher-order schemes to solve the problem. We refer readers to [40–42] for further studies.

In [43], the stability of the fractional DDEs

$$\begin{aligned} {}^{c}\mathcal{D}_t^{\kappa}(u)(t) &= f(t,u_t), \quad t \in [0,b], \kappa \in (0,1), \\ u(t) &= w(t), \qquad t \in [-d,0], \end{aligned} \tag{2}$$

is investigated in the sense of Ulam–Hyers stability. Here, $f : [0,b] \times C([-d,0],\mathbb{R}^m) \to \mathbb{R}^m$ is a continuous function and $u_t(\theta) = u(t+\theta)$, $\theta \in [-d,0]$. The following theorem states the stability of the fractional DDEs (2).

Theorem 1 (cf. [43]). *Assume that $f : [0,b] \times C \to \mathbb{R}^m$ is a continuous function that fulfills a Lipschitz condition as follows:*

$$\|f(t,u) - f(t,v)\|_C \leq L\|u - v\|, \qquad u,v \in C, t \in [0,b].$$

For every $\epsilon > 0$, if $\bar{u} : [-d,b] \to \mathbb{R}^m$ in the Banach space $C([-d,b],\mathbb{R}^m)$ satisfies

$$\|{}^{c}\mathcal{D}_t^{\kappa}(\bar{u})(t) - f(t,\bar{u}_t)\| \leq \epsilon, \qquad t \in [0,b],$$

then there exists a unique solution $u : [-d,b] \to \mathbb{R}^m$ of Equation (2) in $C([-d,b],\mathbb{R}^m)$ with $u(0) = \bar{u}(0)$, such that

$$\|\bar{u}(t) - u(t)\| \leq \left(\frac{E_{\kappa}(Lb^{\kappa} - 1}{L}\right)\epsilon, \quad t \in [-d,b],$$

where $E_{\kappa}(t)$ denotes the one-parameter Mittag-Leffler function.

In this study, we attempt to present a novel and accurate algorithm for solving Equation (1). After converting Equation (1) into a Volterra integral equation, the next step is to solve it using the collocation method that relies on the Chebyshev cardinal functions (CCFs). It should be noted that there are many numerical methods for solving integral

equations [44–46], but CCFs are used in this work. The CCFs are the powerful bases for solving a variety of equations [8,10,13]. In this work, the CCFs obtained from the Lobatto grid are used for the first time. Notably, the Lobatto grid is popular for solving boundary value problems.

The upcoming portions of the document are arranged as follows: Section 2 contains a review and introduction of CCFs and their properties. The collocation method is applied to solve fractional DDEs using CCF in Section 3. This section includes an investigation of the convergence analysis as well. Section 4 is dedicated to illustrating the accuracy and applicability of the method. To sum up the work, a conclusion is included in Section 5.

2. Chebyshev Cardinal Polynomials Based on the Lobatto Grid

Let us denote the Chebyshev polynomials of the order N by C_N. As we know, C_N has N real, simple, and different roots, sometimes called Chebyshev nodes. The Chebyshev nodes can be set as $\{t_n\}_{n=1}^{N}$. Defining the Chebyshev polynomials onto the interval $[a,b]$, called shifted Chebyshev polynomials and characterized by C_N^*, is easy, and can be performed by an affine transformation $t \mapsto \frac{2(t-a)}{b-a} - 1$ that maps $[-1,1]$ into $[a,b]$, viz.

$$C_N^*(t) := C_N\left(\frac{2(t-a)}{b-a} - 1\right). \tag{3}$$

Consequently, the roots of C_N^* are obtained through

$$t_n^* = \frac{1}{2}(t_n + 1)(b-a) + a, \quad \forall 1 \le n \le N. \tag{4}$$

The CCFs are defined relying on two types of grids of the Chebyshev nodes. The first definition is associated with the Gauss–Chebyshev nodes of C_{N+1}^*, and the second involves the Lobatto grid, which includes the extrema of the Chebyshev polynomial C_N^* along with the endpoints. Considering $\mathcal{D}_t$ as the derivative operator with respect to t, the CCFs corresponding to the Gauss–Chebyshev grid [8,10,47] are stated by

$$B_n(t) = \frac{C_{N+1}^*(t)}{\mathcal{D}_t(C_{N+1}^*)(t_n^*)(t - t_n^*)}, \quad t \in [a,b],\ 1 \le n \le N+1. \tag{5}$$

As mentioned above, there is another definition of CCFs with a substitute of nodes, namely, Lobatto grid, which are determined as

$$B_n(t) = \frac{X(t)\mathcal{D}_t(C_N^*)(t)}{\mathcal{D}_t(XC_N^*)(t_n^*)(t - t_n^*)}, \quad t \in [a,b],\ 1 \le n \le N+1, \tag{6}$$

in which $X(t) = 1 - (\frac{2(t-a)}{b-a} - 1)^2$.

For $\nu \in \mathbb{N}$, the Sobolev space $\mathcal{H}^\nu([a,b])$ is denoted by

$$\mathcal{H}^\nu([a,b]) = \left\{u \in C^\nu([a,b]) : \mathcal{D}_t^\sigma u \in L^2([a,b]), \sigma \le \nu, \sigma \in \mathbb{N}_0\right\},$$

endowed with the inner product

$$(u_1, u_2)_{\mathcal{H}^\nu([a,b])} = \sum_{\sigma=0}^{\nu} (\mathcal{D}_t^\sigma(u_1), \mathcal{D}_t^\sigma(u_2))_{L^2([a,b])}, \tag{7}$$

which induces the norm

$$\|u\|^2_{\mathcal{H}^\nu([a,b])} = \sum_{\sigma=0}^{\nu} \|\mathcal{D}_t^\sigma(u)(t)\|_2^2, \tag{8}$$

and the semi-norm

$$|u|^2_{\mathcal{H}^{\nu,N}([a,b])} = \sum_{\sigma=\min\{\nu,N\}}^{N} \|\mathcal{D}_t^{\sigma}(u)(t)\|_2^2. \tag{9}$$

The remarkable characteristic of the CCFs is their cardinality, i.e.,

$$B_n(t_{n'}) = \delta_{nn'}, \qquad 1 \le n, n' \le N+1, \tag{10}$$

where $\delta_{nn'}$ denotes the Kronecker delta. The significance of this property lies in its ability to help determine coefficients without the need for calculating integrals when approximating any function $u \in \mathcal{H}^{\nu}([a,b])$ with them. Introducing a projection operator $\mathcal{Q}_N$ is essential to map $u \in C[a,b]$ into P_{N+1} (the space of all polynomials of a degree less than $N+1$), i.e.,

$$u(t) \approx \mathcal{Q}_N(u)(t) = \sum_{n=1}^{N+1} u(t_n^*) B_n(t) \in P_{N+1}. \tag{11}$$

Lemma 1 (cf [48]). *Given $N \ge 0$, if $u \in \mathcal{H}^{\nu}([a,b])$, then one has*

$$\|u - \mathcal{Q}_N(u)\|_2 \le C(b-a)^{\nu} N^{-\nu} |u|_{\mathcal{H}^{\nu,N}([a,b])}, \tag{12}$$

where C is a constant independent of N.

2.1. Matrix Representation of the Derivative Operator in CCFs Obtained by Lobatto Grids

Consider $\mathbf{B}(t)$ as a vector function whose components are $\{B_n\}_{1\le n\le N+1}$. The focus of this part is to specify a square matrix D, denoted as

$$\mathcal{D}_t(\mathbf{B})(t) = D\mathbf{B}(t). \tag{13}$$

The process below outlines how to specify the entries for D. Thanks to Equation (11), it is easy to confirm that

$$[D]_{n,n'} = \mathcal{D}_t(B_n)(t_{n'}^*). \tag{14}$$

According to the definition of the CCFs using the Lobatto grid, an alternate formulation can be presented as follows (see, e.g., [9]):

$$B_n(t) = \varkappa_n \prod_{\substack{n'=1 \\ n'\ne n}}^{N+1} (t - t_{n'}^*), \tag{15}$$

where

$$\varkappa_n = \frac{-4\Gamma(2N-2)}{(b-a)^{N+1}\Gamma^2(N-1)\big(\mathcal{D}_t(XT_N^*)(t_n^*)\big)}.$$

Motivated by (6), taking a derivative from both sides of (15) leads to

$$\mathcal{D}_t(B_n)(t) = \varkappa_n \prod_{\substack{n'=1 \\ n'\ne n}}^{N+1} \mathcal{D}_t(t - t_{n'}^*). \tag{16}$$

- If $n = n'$, then we obtain

$$\mathcal{D}_t(B_n)(t) = \varkappa_n \sum_{\substack{n''=1 \\ n''\neq n}}^{N+1} \prod_{\substack{n'=1 \\ n'\neq n,n''}}^{N+1} (t - t^*_{n'}) = \sum_{\substack{n''=1 \\ n''\neq n}}^{N+1} \frac{B_n(t)}{(t - t^*_{n''})}. \tag{17}$$

From Equation (10), it follows that

$$\mathcal{D}_t(B_n)(t^*_{n'}) = \sum_{\substack{n''=1 \\ n''\neq n}}^{N+1} \frac{1}{(t_{n'} - t_{n''})}. \tag{18}$$

- If $n \neq n'$, then one can obtain

$$\mathcal{D}_t(B_n)(t^*_{n'}) = \varkappa_n \prod_{\substack{n''=1 \\ n''\neq n,n'}}^{N+1} (t^*_{n'} - t^*_{n''}). \tag{19}$$

2.2. Matrix Representation of the Fractional Integral Operator in CCFs Obtained by Lobatto Grids

Recalling the fractional integral operator (FIO) (see, e.g., [49,50]),

$$\mathcal{I}^{\kappa}_0(u)(t) = \frac{1}{\Gamma(\kappa)} \int_0^t (t-s)^{\kappa-1} u(s) ds, \quad t \in [0, b], \quad \kappa \in \mathbb{R}^+, \tag{20}$$

the square matrix I_κ fulfills

$$\mathcal{I}^{\kappa}_0(\mathbf{B}(t)) \approx I_\kappa \mathbf{B}(t), \quad t \in (0, b). \tag{21}$$

Thanks to (11), one can calculate the elements of I_κ, as

$$[I_\kappa]_{n,n'} = \mathcal{I}^{\kappa}_0(B_n(t^*_{n'})). \tag{22}$$

For simplicity, the alternate formula of (15) can be considered as [8]

$$B_n(t) = \varkappa_n \prod_{\substack{n'=1 \\ n'\neq n}}^{N+1} (t - t^*_{n'}) = \varkappa_n \sum_{n'=0}^{N} \varrho_{n,n'} t^{N-n'} \tag{23}$$

where

$$\varrho_{n,0} = 1, \varrho_{n,n'} = \frac{1}{n'} \sum_{n''=0}^{n'} \varsigma_{n,n''} \varrho_{n,n'-n''}, \ n' = 1, \ldots, N, n = 1, \ldots, N+1,$$

with

$$\varsigma_{n,n''} = \sum_{\substack{i=1 \\ i\neq n}}^{N+1} (t^*_i)^{n''}, \ n'' = 1, \ldots, N, n = 1, \ldots, N+1.$$

Taking into account Property 2.1 [49], and using (23), one can write

$$\begin{aligned}\mathcal{I}_0^{\kappa}(B_n(t)) &= \varkappa_n \mathcal{I}_0^{\mu}\Big(\sum_{n'=0}^{N} \varrho_{n,n'} t^{N-n'}\Big)\\ &= \varkappa_n \sum_{n'=0}^{N} \varrho_{n,n'} \mathcal{I}_0^{\kappa}(t^{N-n'})\\ &= \varkappa_n \sum_{n'=0}^{N} \varrho_{n,n'} \frac{(N-n')!}{\Gamma(N-n'+\kappa+1)} t^{N-n'+\kappa}.\end{aligned} \tag{24}$$

Consequently, (22) and (24) lead to determining

$$[I_\kappa]_{n,n'} = \varkappa_n \sum_{n'=0}^{N} \varrho_{n,n'} \frac{(N-n')!}{\Gamma(N-n'+\kappa+1)} (t_{n'}^*)^{N-n'+\kappa}. \tag{25}$$

3. Proposed Algorithm

Converting an ODE to the corresponding integral equation and solving it is a common technique. Fractional ODEs can benefit from the utilization of this technique as well. Achieving this is possible with the use of [49]

$$\mathcal{I}_0^{\kappa c}\mathcal{D}_t^{\kappa}(u)(t) = u(t) - \sum_{i=0}^{\lceil\kappa\rceil-1} \frac{\mathcal{D}_t^i(u)(0)}{i!} t^i, \tag{26}$$

where $\lceil . \rceil$ indicates the ceiling function. Taking into account (1) and using (26), one can derive the corresponding integral equation of (1)

$$u(t) - y(t) = \mathcal{I}_0^{\kappa}(u(s-d) + u(s) + g(s))(t), \tag{27}$$

in which $y(t) = \sum_{i=0}^{\lceil\kappa\rceil-1} \frac{\mathcal{D}_t^i(u)(0)}{i!} t^i$. The equivalence of the solutions of (1) and (27) is discussed previously (see, e.g., [49]).

The first step in our scheme is to approximate the unknown solution u by CCFs, viz.,

$$u(t) \approx \mathcal{Q}_N(u)(t) = \sum_{n=1}^{N+1} u_n B_n(t) = u_N(t). \tag{28}$$

For the term $u(t-d)$, considering the delay condition, one can write

$$u(t-d) = \begin{cases} w(t-d), & t \in [0,d],\\ u(t-d), & t \in (d,1]. \end{cases} \tag{29}$$

Using (28) and (29), one can approximate $u(t-d)$ as

$$u(t-d) := \tilde{u}(t) \approx \sum_{n=1}^{N+1} \tilde{u}_n B_n(t) = \tilde{u}_N(t). \tag{30}$$

Substituting u_N in integral Equation (27) leads to

$$u_N(t) - y_N(t) = \mathcal{I}_0^{\kappa}(\tilde{u}_N(s) + u_N(s) + g_N(s))(t), \tag{31}$$

where $y_N(t) = \mathcal{Q}_N(y)(t)$ and $g_N(t) = \mathcal{Q}_N(g)(t)$.

The collocation approach serves as the cornerstone of the proposed algorithm. It is important to note that the collocation method opts for the solution that satisfies the

equation conditions at the collocation points. Equivalently, the residual function $r(t)$ must approach zero at the collocation points. The residual function can be introduced as follows:

$$r(t) = u_N(t) - y_N(t) - \mathcal{I}_0^{\kappa}(\tilde{u}_N(s) + u_N(s) + g_N(s))(t). \tag{32}$$

Thanks to the matrix representation of FIO, and using the Lobatto grid as the collocation points, the following linear system can be obtained:

$$r(t_n^*) = 0, \qquad 1 \le n \le N+1, \tag{33}$$

or equivalently,

$$u_N(t_n^*) - y_N(t_n^*) - \mathcal{I}_0^{\kappa}(\tilde{u}_N(s) + u_N(s) + g_N(s))(t_n^*) = 0, \qquad 1 \le n \le N+1. \tag{34}$$

Solving this system leads to finding the unknowns $\{u_n\}_{n=1}^{N+1}$.

3.1. Convergence Analysis

The boundedness of the FIO in $L^p[a,b]$ is presented in [49] as

$$\|\mathcal{I}_0^{\kappa}(u)\|_p \le K\|u\|_p, \qquad \text{with} \qquad K = \frac{(b-a)^{\kappa}}{\Gamma(\kappa+1)}. \tag{35}$$

Theorem 2. *Given $N, \nu \in \mathbb{N}$, assume that $u \in \mathcal{H}^{\nu}([0,b])$. The proposed method is convergence and the error satisfies*

$$\|e_N\|_{L^2[0,b]} \le KC\Lambda N^{-\nu} b^{\nu} |u|_{\mathcal{H}^{\nu,N}[0,b]},$$

where C, K are constants, and $\Lambda = \max\{|\tilde{u}|_{\mathcal{H}^{\nu,N}[0,b]}, |g|_{\mathcal{H}^{\nu,N}[0,b]}\}$.

Proof. Let $e_N = u - u_N$. Subtracting Equation (27) from (31) leads to

$$e_N(t) = y(t) - y_N(t) + \mathcal{I}_0^{\kappa}(\tilde{u}(s) - \tilde{u}_N(s) + u(s) - u_N(s) + g(s) - g_N(s))(t). \tag{36}$$

Motivated by Lemma 1 and using (35), we obtain

$$\|\mathcal{I}_0^{\kappa}(\tilde{u}(s) - \tilde{u}_N(s))(t)\|_{L^2[0,b]} \le K\|\tilde{u}(t) - \tilde{u}_N(t)\|_{L^2[0,b]}. \tag{37}$$

Taking into account the definition of $\tilde{u}(t)$, it follows that

$$\|\tilde{u}(t) - \tilde{u}_N(t)\|^2_{L^2[0,b]} \le \|\tilde{w}(t) - \tilde{w}_N(t)\|^2_{L^2[-d,0]} + \|u(t) - u_N(t)\|^2_{L^2[0,b]}. \tag{38}$$

Thus, it is concluded that

$$\begin{aligned} \|\mathcal{I}_0^{\kappa}(\tilde{u}(s) - \tilde{u}_N(s))(t)\|_{L^2[0,b]} &\le K\Big(\|\tilde{w}(t) - \tilde{w}_N(t)\|_{L^2[-d,0]} + \|u(t) - u_N(t)\|_{L^2[0,b]}\Big) \\ &\le KCN^{-\nu}\Big(d^{\nu}|w|_{\mathcal{H}^{\nu,N}([-d,0])} + b^{\nu}|u|_{\mathcal{H}^{\nu,N}([0,b])}\Big). \end{aligned} \tag{39}$$

Similarly,

$$\begin{aligned} \|\mathcal{I}_0^{\kappa}(e_N(t))\|_{L^2[0,b]} &\le K\|e_N(t)\|_{L^2[0,b]} \le KCN^{-\nu} b^{\nu} |u|_{\mathcal{H}^{\nu,N}([0,b])}, \\ \|\mathcal{I}_0^{\kappa}(g(s) - g_N(s))(t)\|_{L^2[0,b]} &\le K\|g(t) - g_N(t)\|_{L^2[0,b]} \le KCN^{-\nu} b^{\nu} |g|_{\mathcal{H}^{\nu,N}([0,b])}. \end{aligned} \tag{40}$$

Taking the L^2-norm from both sides of (36), and utilizing (37)–(40), one can obtain

$$\|e_N(t)\|_{L^2[0,b]} \le KCN^{-\nu} b^{\nu}\Big(|w|_{\mathcal{H}^{\nu,N}([-d,0])} + |u|_{\mathcal{H}^{\nu,N}([0,b])} + |g|_{\mathcal{H}^{\nu,N}([0,b])}\Big).$$

Putting $\Lambda = \max\{|w|_{\mathcal{H}^{\nu,N}[-d,0]}, |g|_{\mathcal{H}^{\nu,N}[0,b]}\}$, one can obtain

$$\|e_N\|_{L^2[0,b]} \leq KC\Lambda N^{-\nu} b^{\nu} |u|_{\mathcal{H}^{\nu,N}[0,b]}. \tag{41}$$

□

3.2. Stability Analysis

Let us rewrite Equation (34) as

$$\mathcal{L}(u_N)(t_n^*) = f(t_n^*), \qquad 1 \leq n \leq N+1, \tag{42}$$

where

$$\mathcal{L}(u_N)(t_n^*) := u_N(t_n^*) - \mathcal{I}_0^{\kappa}(\tilde{u}_N(s) + u_N(s))(t_n^*),$$
$$f(t_n^*) := y_N(t_n^*) - \mathcal{I}_0^{\kappa}(g_N(s))(t_n^*).$$

The coefficient matrix of system (42) can be rewritten as

$$\begin{pmatrix} \mathcal{L}(B_1)(t_1^*) & \dots & \mathcal{L}(B_{N+1})(t_1^*) \\ \vdots & \ddots & \vdots \\ \mathcal{L}(B_1)(t_{N+1}^*) & \dots & \mathcal{L}(B_{N+1})(t_{N+1}^*) \end{pmatrix} \begin{pmatrix} u_1 \\ \vdots \\ u_{N+1} \end{pmatrix} = \begin{pmatrix} f(t_1^*) \\ \vdots \\ f(t_{N+1}^*) \end{pmatrix}. \tag{43}$$

Denote

$$A = \begin{pmatrix} \mathcal{L}(B_1)(t_1^*) & \dots & \mathcal{L}(B_{N+1})(t_1^*) \\ \vdots & \ddots & \vdots \\ \mathcal{L}(B_1)(t_{N+1}^*) & \dots & \mathcal{L}(B_{N+1})(t_{N+1}^*) \end{pmatrix}$$

Assume λ is a eigenvalue of the matrix A. Therefore, there exists a vector $X \in \mathbb{R}^{N+1}$ such that $(A - \lambda I)X = 0$. Hence,

$$\lambda x_j = \sum_{i=1}^{N+1} \mathcal{L}(B_i(t_j^*))x_i, \qquad j = 1, \dots N+1.$$

Multiplying both sides by x_j and then taking the summation $\sum_{j=1}^{N+1}$ leads to

$$\lambda \sum_{j=1}^{N+1} x_j^2 = \sum_{j=1}^{N+1} \sum_{i=1}^{N+1} \mathcal{L}(B_i(t_j^*))x_i x_j.$$

Thus, we have

$$\begin{aligned} \lambda &= \sum_{j=1}^{N+1} \sum_{i=1}^{N+1} \mathcal{L}(B_i(t_j^*))x_i \frac{x_j}{\|X\|_2^2}, \\ &= \sum_{j=1}^{N+1} \mathcal{L}\left(\sum_{i=1}^{N+1} B_i(t_j^*)x_i \right) \frac{x_j}{\|X\|_2^2}, \\ &= \sum_{j=1}^{N+1} \mathcal{L}(v(t_j^*)) \frac{x_j}{\|X\|_2^2}, \qquad \left(v(t) = \sum_{i=1}^{N+1} x_i B_i(t) \right). \end{aligned}$$

It follows from (10) that

$$\lambda_{\max} = \| \sum_{j=1}^{N+1} \mathcal{L}(v(t_j^*)) \frac{x_j}{\|X\|_2^2} \|_{\infty} \leq \|\mathcal{L}\|_{\infty} \| \sum_{j=1}^{N+1} v(t_j^*) \frac{x_j}{\|X\|_2^2} \|_{\infty} \leq \|\mathcal{L}\|_{\infty}. \tag{44}$$

It is not hard to verify that $\lambda_{\min} \geq \frac{1}{\|\mathcal{L}\|_\infty}$. To this end, suppose that there is a $v(t)$, with $\| \sum_{j=1}^{N+1} v(t_j^*) \frac{x_j}{\|X\|_2^2} \|_\infty = 1$ such that $\| \sum_{j=1}^{N+1} \mathcal{L}(v(t_j^*)) \frac{x_j}{\|X\|_2^2} \|_\infty < \frac{1}{\|\mathcal{L}\|_\infty}$. Denote $z = \mathcal{L}\left(\sum_{j=1}^{N+1} v(t_j^*) \frac{x_j}{\|X\|_2^2} \right)$. Hence, $\|z\| < \frac{1}{\|\mathcal{L}\|_\infty}$. Thus, one can verify that

$$1 = \| \sum_{j=1}^{N+1} v(t_j^*) \frac{x_j}{\|X\|_2^2} \|_\infty = \|\mathcal{L}^{-1}(z)\|_\infty \leq \|\mathcal{L}^{-1}\|_\infty \|z\|_\infty < \|\mathcal{L}^{-1}\|_\infty \frac{1}{\|\mathcal{L}\|_\infty} = 1$$

This is a contradiction, and therefore, we have $\lambda_{\min} \geq \frac{1}{\|\mathcal{L}\|_\infty}$.

As a result, one can write

$$1 \leq Cond(A) = \frac{\lambda_{\max}}{\lambda_{\min}} \leq \|\mathcal{L}\|_\infty \|\mathcal{L}^{-1}\|_\infty.$$

Motivated by [51], the operator $\mathcal{L}$ and its inverse are bounded operators. This implies that the spectral condition number of the matrix A is bounded, and the proposed algorithm is stable.

4. Numerical Experiments

Theoretical results from earlier sections are depicted here. To this end, we consider some examples whose analytical solution is known.

Example 1. *Consider the fractional DDE as follows [40,41]:*

$$\begin{aligned} {}^c\mathcal{D}_t^{0.3}(u)(t) &= u(t-1) - u(t) + 3t^2 - 3t + 1 + \frac{\Gamma(4)}{\Gamma(4-0.3)} t^{2.7}, \quad t \in [0,1], \\ u(t) &= t^3, \qquad t \in [-1,0]. \end{aligned}$$

The analytic solution for this equation is reported in [40] as $u(t) = t^3$.

Table 1 tabulates the absolute error obtained via the presented method. It compares the results with the Haar wavelet collocation method [40] and the fractional backward difference method [41]. As mentioned in the previous section, the method is convergent. Thus, we expect the error to decrease when the number of bases increases. Figure 1 illustrates that the method is convergent and verifies our investigation in the previous section. The numerical solution and the corresponding errors are plotted in Figure 2. The order of convergence is reported in Table 2.

Table 1. The errors obtained by the presented method for Example 1.

N	Presented Method	N	Results of [40]	N	Results of [41]
4	4.49×10^{-4}	4	5.85×10^{-3}	10	7.11×10^{-2}
6	1.61×10^{-5}	8	2.61×10^{-3}	20	4.12×10^{-2}
8	2.64×10^{-6}	16	9.78×10^{-4}	40	2.20×10^{-2}
10	4.63×10^{-7}	32	3.40×10^{-4}	80	1.13×10^{-2}

Table 2. The order of convergence for Example 1.

N	2	4	8	16	32	64	128
L^2-error	3.39×10^{-1}	2.92×10^{-4}	1.56×10^{-6}	1.52×10^{-8}	1.70×10^{-10}	1.85×10^{-12}	2.03×10^{-14}
Order	–	10.1811	7.5483	6.6813	6.4866	6.5176	6.5099

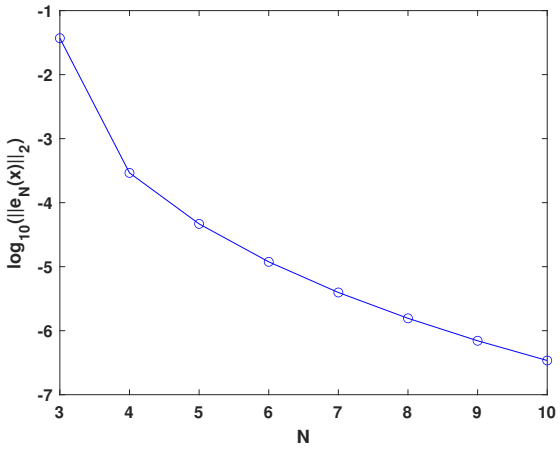

Figure 1. The errors reported for different values of N (Example 1).

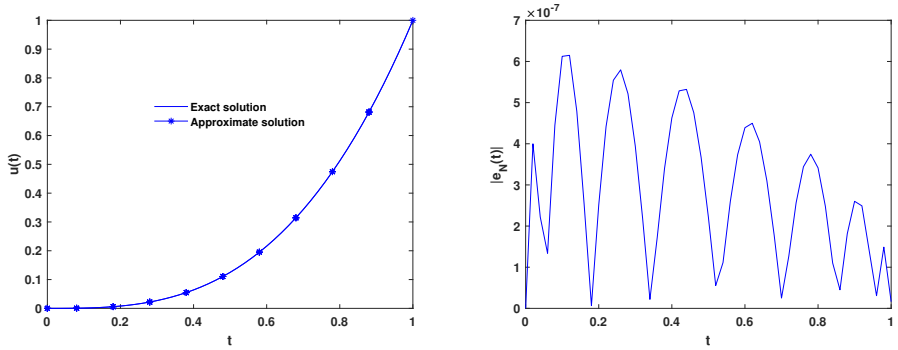

Figure 2. The plot of a numerical solution (**left**) and the corresponding error (**right**) with $N = 10$ (Example 1).

Example 2. *Consider the fractional DDE as follows [28,40,41]:*

$$
\begin{aligned}
{}^{c}\mathcal{D}_{t}^{0.5}(u)(t) &= u(t-1) - u(t) + 2t - 1 + \frac{2}{\Gamma(5/2)}t^{3/2}, \quad t > 0, \\
u(t) &= t^2, \qquad t \in [-1, 0].
\end{aligned}
$$

Motivated by [28], the analytic solution is $u(t) = t^2$.

The absolute error obtained via the presented method is reported in Table 3. A comparison is made between the presented method and the methods reported in [40,41]. Figure 3 illustrates the method is convergent, and verifies our investigation in the previous section. The numerical solution and the corresponding errors are plotted in Figure 4. The order of convergence is reported in Table 4.

Table 3. Errors obtained by the presented method for Example 2.

N	**Presented Method**	N	**Results of [40]**	N	**Results of [41]**
6	1.40×10^{-4}	4	7.11×10^{-3}	10	4.92×10^{-2}
8	3.80×10^{-5}	8	2.81×10^{-3}	20	2.76×10^{-2}
10	1.40×10^{-5}	16	1.07×10^{-3}	40	1.47×10^{-2}
12	6.25×10^{-6}	32	3.96×10^{-4}	80	7.56×10^{-3}

Table 4. Order of convergence for Example 2.

N	2	4	8	16	32	64
L^2-error	2.19×10^{-1}	9.38×10^{-4}	3.80×10^{-5}	1.75×10^{-6}	8.21×10^{-8}	3.87×10^{-9}
Order	–	7.8671	4.6255	4.4406	4.4138	4.3734

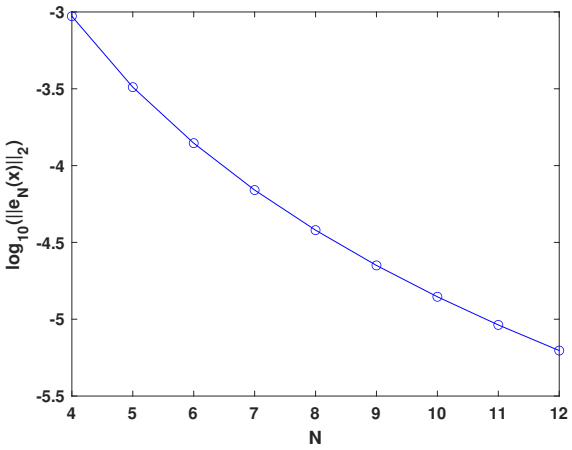

Figure 3. Errors reported for different values of N (Example 2).

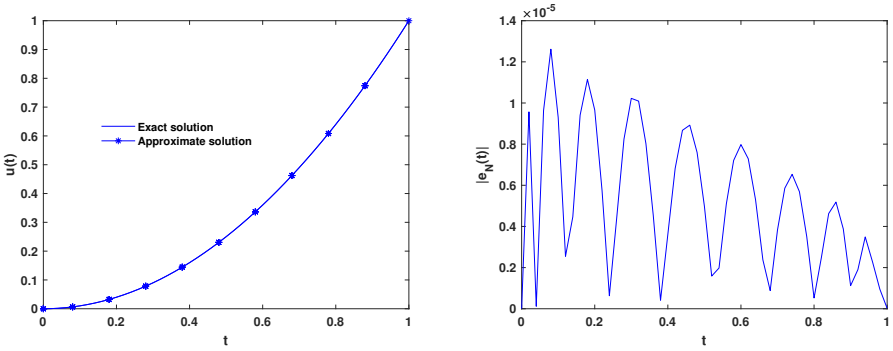

Figure 4. Plot of a numerical solution (**left**) and the corresponding error (**right**) with $N = 12$ (Example 2).

Example 3. *Consider the following fractional DDE [36]:*

$$\begin{aligned} {}^{c}\mathcal{D}_t^{\kappa}(u)(t) &= -u(t-1), \quad 0 < t \leq 4, \\ u(t) &= 1, \qquad t \leq 0. \end{aligned}$$

The exact solution for this equation is not available. However, for the special case when $\kappa = 1$, the exact solution is reported in [36] as

$$\begin{cases} 1 - x, & 0 < x \leq 1, \\ \frac{1}{2}x^2 - 2x + \frac{3}{2}, & 1 < x \leq 2, \\ -\frac{1}{6}x^3 + \frac{3}{2}x^2 - 4x + \frac{17}{6}, & 2 < x \leq 3, \\ \frac{1}{24}x^4 - \frac{2}{3}x^3 + \frac{15}{4}x^2 - \frac{17}{2}x + \frac{149}{24}, & 3 < x \leq 4. \end{cases}$$

Figure 5 demonstrates the method is convergent, and verifies our investigation in the previous section. To confirm the ability of the method to solve the fractional DDE, Figure 6 is plotted. It can be seen that as κ approaches 1, the approximate solution approaches the results for $\kappa = 1$.

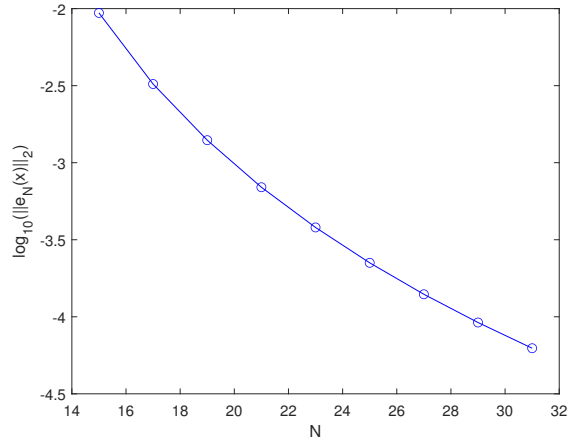

Figure 5. Errors reported for different values of N (Example 3).

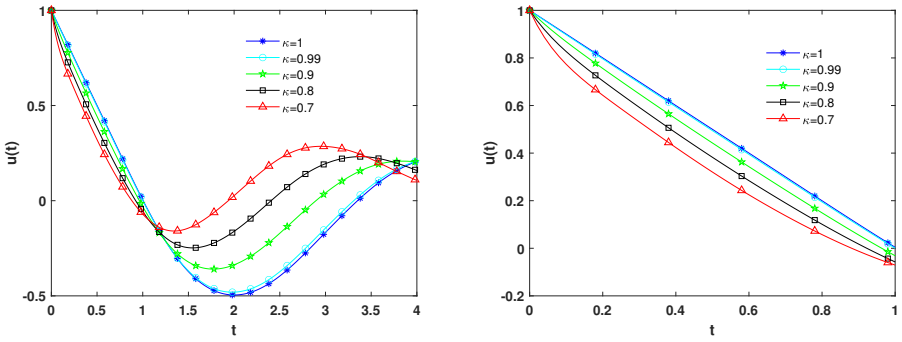

Figure 6. Approximate solutions for different choices of κ, taking $N = 15$ (Example 3).

Example 4. *Consider the following fractional DDE [41]:*

$$\begin{aligned} {}^{c}\mathcal{D}_{t}^{\kappa}(u)(t) &= u(t-1) - t, \quad 0 < t \leq 2, \\ u(t) &= t, \qquad t \in [-1, 0]. \end{aligned}$$

The exact solution for this equation is reported in [41] as

$$u(t) = \begin{cases} -\frac{2\sqrt{x}}{\sqrt{\pi}}, & 0 \leq x \leq 1, \\ \frac{2\left(\sqrt{x-1}-\sqrt{x}\right)}{\sqrt{\pi}} + 1 - x - \frac{2\sqrt{x-1}\cdot(1+2x)}{3\sqrt{\pi}}, & 1 \leq x \leq 2. \end{cases}$$

The L^2- error and the order of convergence are reported in Table 5. This table shows the accuracy and ability of the presented method. As you can see, the error decreases as the number of bases increases. The numerical solution and the corresponding errors are plotted in Figure 7.

Table 5. Order of convergence for Example 4.

N	4	8	16	32	64	128	25
L^2-error	1.96×10^{-1}	6.70×10^{-2}	1.45×10^{-2}	3.57×10^{-3}	8.86×10^{-4}	2.20×10^{-4}	5.554×10^{-5}
Order	–	1.5486	2.2081	2.0215	2.0112	2.0085	1.9895

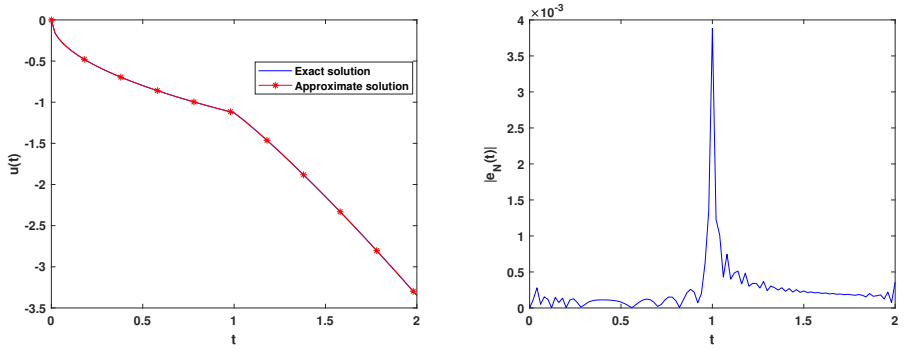

Figure 7. Plot of numerical solution (**left**) and corresponding error (**right**) with $N = 128$ (Example 4).

5. Conclusions

According to the important role of fractional DDEs in various fields of science, introducing novel and efficient schemes for solving them can be valuable. This is the main focus of the study. The algorithm presented improves the accuracy and efficiency of the collocation method. The algorithm is derived by reducing the equation to the Volterra integral equation and solving this integral equation with the collocation method. To confirm the convergence of the method, we performed a rigorous analysis, and the numerical examples support our findings.

Based on the experimental observations, the following conclusions can be drawn:

- The presented algorithm demonstrates efficiency in solving the fractional DDEs.
- Our algorithm demonstrates convergence when tackling these equations.
- The method presented offers reduced computational cost by avoiding integration to find coefficients.
- The CCFs based on the Lobatto grid can efficiently be used as the bases in the spectral methods, especially when studying boundary value equations.
- The proposed algorithm is simple to implement, and it also provides good accuracy.

Author Contributions: Conceptualization, H.B.J. and I.D.; methodology, H.B.J.; software, H.B.J. and I.D.; validation, H.B.J. and I.D.; formal analysis, H.B.J. and I.D.; investigation, H.B.J. and I.D.; writing—original draft preparation, H.B.J. and I.D.; writing—review and editing, H.B.J. and I.D.; visualization, H.B.J. and I.D.; supervision, H.B.J.; project administration, H.B.J. and I.D.; funding acquisition, H.B.J. All authors have read and agreed to the published version of the manuscript.

Funding: This project was supported by Researchers Supporting Project number RSP2024R210, King Saud University, Riyadh, Saudi Arabia.

Data Availability Statement: The original contributions presented in the study are included in the article, further inquiries can be directed to the corresponding author.

Conflicts of Interest: The writers state that they have no known personal relationships or competing financial interests that could have appeared to affect the work reported in this work.

Nomenclature

${}^{c}\mathcal{D}_t^{\kappa}$	Caputo fractional derivative
L	Lipschitz constant
E_{κ}	one-parameter Mittag-Leffler function
C_N	Chebyshev polynomials
C_N^*	shifted Chebyshev polynomials
B_n	Chebyshev cardinal functions
$\mathcal{H}^{\nu}$	Sobolev space
$\mathcal{Q}_N$	projection operator
$\mathcal{D}_t$	derivative operator with respect to t
$\mathcal{I}_0^{\kappa}$	fractional integral operator

References

1. Arif, M.; Ali, F.; Khan, I.; Nisar, K.S. A time fractional model with non-singular kernel the generalized couette flow of couple stress nanofluid. *IEEE Access* **2020**, *8*, 77378–77395. [CrossRef]
2. Chang, A.; Sun, H.; Zheng, C.; Bingqing, L.; Chengpeng, L.; Rui, M.; Yong, Z. A Time Fractional Convection-Diffusion Equation to Model Gas Transport through Heterogeneous Soil and Gas Reservoirs. *Physica A* **2018**, *502*, 356–369. [CrossRef]
3. Tenreiro, M.; Silva M.F.; Barbosa R.S.; Jesus I.S.; Reis Cecília, M.; Marcos M.G.; Galhano, A.F. Some Applications of Fractional Calculus in Engineering. *Math. Probl. Eng.* **2010**, *2010*, 639801 . [CrossRef]
4. Mainardi, F. *Fractional Calculus and Waves in Linear Viscoelasticity*; Imperial College Press: London, UK, 2010.
5. Asadzadeh, M.; Saray, B.N. On a multiwavelet spectral element method for integral equation of a generalized Cauchy problem. *BIT* **2022**, **62**, 383–1416. [CrossRef]
6. Shi, L.; Saray B.N.; Soleymani, F. Sparse wavelet Galerkin method: Application for fractional Pantograph problem. *J. Comput. Appl. Math.* **2024**, *451*, 116081. [CrossRef]
7. Thanh Toan, P.; Vo, T.N.; Razzaghi, M. Taylor wavelet method for fractional delay differential equations. *Eng. Comput.* **2021**, *37*, 231–240. [CrossRef]
8. Afarideh, A.; Dastmalchi Saei, F.; Lakestani, M.; Saray, B.N. Pseudospectral method for solving fractional Sturm-Liouville problem using Chebyshev cardinal functions. *Phys. Scr.* **2021**, *96*, 125267. [CrossRef]
9. Afarideh, A.; Dastmalchi Saei, F.; Saray, B.N. Eigenvalue problem with fractional differential operator: Chebyshev cardinal spectral method. *J. Math. Model.* **2021**, *11*, 343–355.
10. Shahriari, M.; Saray, B.N.; Mohammadalipour, B.; Saeidian, S. Pseudospectral method for solving the fractional one-dimensional Dirac operator using Chebyshev cardinal functions. *Phys. Scr.* **2023**, *98*, 055205. [CrossRef]
11. Garrappa, R. On some explicit Adams multistep methods for fractional differential equations. *J. Comput. Appl. Math.* **2009**, *229*, 392–399. [CrossRef]
12. Lin, Z.; Wang, D.; Qi, D.; Deng, L. A Petrov–Galerkin finite element-meshfree formulation for multi-dimensional fractional diffusion equations. *Comput. Mech.* **2020**, *66*, 323–350. [CrossRef]
13. Lakestani, M.; Dehghan, M. The use of Chebyshev cardinal functions for the solution of a partial differential equation with an unknown time-dependent coefficient subject to an extra measurement. *J. Comput. Appl. Math.* **2010**, *235*, 669–678. [CrossRef]
14. Daftardar-Gejji, V.; Jafari, A. Adomian decomposition: A tool for solving a system of fractional differential equations. *J. Math. Anal. Appl.* **2005**, *301*, 508–518. [CrossRef]
15. Fix G.J.; Roop, J.P. Least squares finite element solution of a fractional order two-point boundary value problem. *Comput. Math. Appl.* **2004**, *48*, 1017–1033. [CrossRef]
16. Zhao YL.; Zhu, P.; Gu, X.M.; Zhao, X.; Jian, H.Y. An implicit integration factor method for a kind of spatial fractional diffusion equations. *J. Phys. Conf. Ser.* **2019**, *1324*, 012030. [CrossRef]
17. Maji, S.; Natesan, S. Adaptive-grid technique for the numerical solution of a class of fractional boundary-value-problems. *Comput. Methods Differ. Equ.* **2010**, *12*, 338–349.
18. Epstein, I.R.; Luo, Y. Differential delay equations in chemical kinetics. Nonlinear models: The cross-shaped phase diagram and the oregonator. *J. Chem. Phys.* **1991**, *95*, 244–254. [CrossRef]
19. Davis, L. Modifications of the optimal velocity traffic model to include delay due to driver reaction time. *Phys. A Stat. Mech. Appl.* **2003**, *319*, 557–567. [CrossRef]
20. Fridman, E.; Fridman, L.; Shustin, E. Steady modes in relay control systems with time delay and periodic disturbances. *J. Dyn. Syst. Meas. Control* **2000**, *122*, 732–737. [CrossRef]
21. Kuang, Y. *Delay Differential Equations: With Applications in Population Dynamics*; Academic Press: London, UK, 1993; Volume 191.
22. Saray B.N.; Lakestani, M. On the sparse multi-scale solution of the delay differential equations by an efficient algorithm. *Appl. Math. Comput.* **2020**, *381*, 125291. [CrossRef]
23. Mohammadzade, R.; Lakestani, M. Analysis of time-varying delay systems by hybrid of block-pulse functions and biorthogonal multiscaling functions. *Int. J. Control.* **2015**, *88*, 2444–2456 [CrossRef]
24. Marzban H.R.; Razzaghi, M. Analysis of time-delay systems via hybrid of block-pulse functions and taylor series. *J. Vib. Control* **2005**, *11*, 1455–1468. [CrossRef]
25. Huang, C.; Fu H.; Li, S.; Chen, G. Stability analysis of Runge-Kutta methods for non-linear delay differential equations. *BIT* **1999**, *39*, 270–280.
26. Kuang, J.; Cong, Y. *Stability of Numerical Methods for Delay Differential Equations*; Science Press: Beijing, China, 2005.
27. Li, D.; Zhang, C. Nonlinear stability of discontinuous Galerkin methods for delay differential equations. *Appl. Math. Lett.* **2010**, *23*, 457–461. [CrossRef]
28. Xu, X.; Huang, Q.; Chen, H. Local Superconvergence vergence of continuous Galerkin solutions for delay differential equations of pantograph type. *J. Comput. Math.* **2016**, *34*, 2664–2684.
29. Zennaro, M. P-stability of Runge-Kutta methods for delay differential equations. *Numer. Math.* **1986**, *49* 305–318. [CrossRef]
30. Zennaro, M. Asymptotic stability analysis of Runge-Kutta methods for nonlinear systems of delay differential equations. *Numer. Math.* **1997**, *77*, 549–563. [CrossRef]
31. Daftardar-Gejji, V. *Fractional Calculus: Theory and Applications*; Narosa Publishing House: New Delhi, India, 2014.

32. Zhen, W.; Xia, H.; Guodong, S. Analysis of nonlinear dynamics and chaos in a fractional order financial system with time delay. *Comput. Math. Appl.* **2011**, *62*, 1531–1539.
33. Singh, H. Numerical simulation forfractional delay differential equations. *Int. J. Dynam. Control* **2021**, *9*, 463–474. [CrossRef]
34. Liao, C.; Ye, H. Existence of positive solutions of nonlinear fractional delay differential equations. *Positivity* **2009**, *13*, 601–609. [CrossRef]
35. Daftardar-Gejji, V.; Sukale, Y.; Bhalekar, S. Solving fractional delay differential equations: A new approach. *Fract. Calc. Appl. Anal.* **2015**, *18*, 400–418. [CrossRef]
36. Dehestani, H.; Ordokhani, Y.; Razzaghi, M. On the applicability of Genocchi wavelet method for different kinds of fractional-order differential equations with delay. *Numer. Linear. Algebr.* **2019** *26*, e2259. [CrossRef]
37. Singh, H.; Pandey R.K.; Baleanu, D. Stable Numerical Approach for Fractional Delay Differential Equations. *Few-Body Syst.* **2017**, *58*, 156. [CrossRef]
38. Jhinga, A.; Daftardar-Gejji, V. A new numerical method for solving fractional delay differential equations. *Comput. Appl. Math.* **2019**, *38*, 166. [CrossRef]
39. Gande N.R.; Madduri, H. Higher order numerical schemes for the solution of fractional delay differential equations. *J. Comput. Appl. Math.* **2022**, *402*, 113810. [CrossRef]
40. Amin, R.; Shah, K.; Asif, M.; Khan, I. A computational algorithm for the numerical solution of fractional order delay differential equations. *Appl. Math. Comput.* **2021**, *402*, 125863. [CrossRef]
41. Morgado M.L.; Ford N.J.; Lima, P. Analysis and numerical methods for fractional differential equations with delay. *J. Comput. Appl. Math.* **2013**, *252*, 159–168. [CrossRef]
42. Xu, M.; Lin, Y. Simplified reproducing kernel method for fractional differential equations with delay. *Appl. Math. Lett.* **2016**, *52*, 156–161 [CrossRef]
43. Kucche K.D.; Sutar, S.T. On existence and stability results for nonlinear fractional delay differential equations. *Bol. Soc. Parana. Mat.* **2018**, *36*, 55–75. [CrossRef]
44. Noeiaghdam, S.; Fariborzi Araghi, M.A.; Sidorov, D. Dynamical strategy on homotopy perturbation method for solving second kind integral equations using the CESTAC method. *J. Comput. Appl. Math.* **2022**, *411*, 114226. [CrossRef]
45. Saray, B.N. Sparse multiscale representation of Galerkin method for solving linear-mixed Volterra-Fredholm integral equations. *Math. Method Appl. Sci.* **2020**, *43*, 2601–2614. [CrossRef]
46. Noeiaghdam, S.; Sidorov, D.; Wawaz, A.-M.; Sidorow, N.; Sizikov, V. The Numerical Validation of the Adomian Decomposition Method for Solving Volterra Integral Equation with Discontinuous Kernels. *Mathematics* **2021**, *9*, 260. [CrossRef]
47. Boyd, J.P. *Chebyshev and Fourier Spectral Methods*, 2nd ed.; Dover Publications: New York, NY, USA , 2001.
48. Shen, J.; Tang, T.; Wang, L.L. *Spectral Methods: Algorithms. Analysis, Applications*; Springer: Berlin/Heidelberg, Germany, 2011.
49. Kilbas, A.; Srivastava H.M.; Trujillo, J.J. *Theory and Applications of Fractional Differential Equations*; Elsevier: Amsterdam, The Netherland, 2006.
50. Saray B.N. Abel's integral operator: Sparse representation based on multiwavelets. *BIT* **2021**, *61*, 587–606. [CrossRef]
51. Shi, L.; Chen, Z.; Ding, X.; Ma, Q. A new stable collocation method for solving a class of nonlinear fractional delay differential equations. *Numer. Algor.* **2020**, *85*, 1123–1153. [CrossRef]